DYNAMICS OF OBJECTIVE STRUCTURES OF THE NANOTUBE GROUP

By

Milka Doktorova

Dhruv Goel

and

Michael Meaden

IMA Preprint Series # 2273

(August 2009)

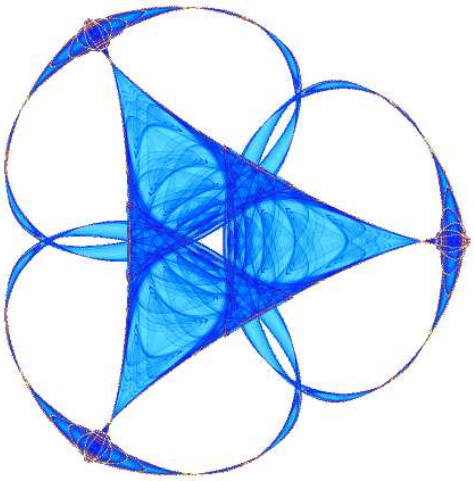

INSTITUTE FOR MATHEMATICS AND ITS APPLICATIONS

UNIVERSITY OF MINNESOTA

400 Lind Hall

207 Church Street S.E.

Minneapolis, Minnesota 55455–0436

Phone: 612/624-6066 Fax: 612/626-7370

URL: http://www.ima.umn.edu

Dynamics of Objective Structures of the Nanotube Group

Milka Doktorova[1], Dhruv Goel[2], Michael Meaden[3]

July 31, 2009

Abstract

An objective structure is a collection of distinct points having identical physical environments. Such structures are produced by applying a discrete subgroup of an isometry group to a finite set of points. Here the objective structures are generated by the nanotube group and their dynamics are simulated using the Lennard-Jones potential and the velocity Verlet method. These structures are defined by the number of points in a ring, n, and the distance and angular displacement between two consecutive rings, τ and α, respectively. In a typical simulation, the radius of the nanotube oscillates due to interparticle forces. Our analysis shows that for $\alpha \neq 0$ objective structures achieve the lowest minimum radius at $\tau = \sigma$ where σ is a parameter for the Lennard-Jones potential. Furthermore, varying τ linearly with time has almost no impact on the minimum radius of the objective structure. Analyzing the minimum radius of the structure versus different values of α reveals minima at $\alpha = 0$ and $\alpha = \frac{\pi}{n}$ with discontinuity at zero.

Introduction

Objective structures are discrete sets of points in $\mathbb{R}^3$ with a particular type of symmetry. They model many structures observed in nature such as viral structures, or manmade objects such as carbon nanotubes. In general,

[1]Mount Holyoke College, Email: dokto20m@gmail.com
[2]University of Minnesota, Email: dhruv@cs.umn.edu
[3]Elmhurst College, Email: meadenm@net.elmhurst.edu

one should think of objective structures as having the property that the same physical environment is observed from any point in the structure [1]. Mathematically, objective structures are produced by applying a discrete subgroup of the affine orthogonal group to a finite set of points.

There are two main types of objective structures: *atomic* and *molecular*. An objective atomic structure is defined as a set of points in $\mathbb{R}^3$ obtained by applying the elements of a given discrete group of isometries to a single point. A molecular objective structure, on the other hand, consists of identical molecules, where each molecule is made up of point masses that may be dissimilar and may not be connected by an isometry. However, the corresponding points in each molecule can be obtained from each other using the transformations or translations from the group and in a way, they form objective atomic structures [1].

Objective structures can be generated either by a single point or by a set of points in a fundamental domain [1]. In both cases the evolution of the structures is modeled by giving an initial velocity to each generating point and using the Lennard-Jones potential to calculate the force exerted on that point by all other points in the structure. The new velocity and position are then calculated with the velocity Verlet method, which allows the structure to move with time.

The molecular dynamics of the structures are the main focus of this research. Following is a summary of the contents of this paper. The first section describes the mathematical foundations of the formation of objective structures. Section 1.1 briefly introduces orthogonal matrices and rotations, while Section 1.2 discusses affine orthogonal groups and isometries. Sections 1.3 and 1.4 introduce the nanotube group and present objective structures obtained by subgroups of the nanotube group.

Section 2 explains the method used for the simulations of molecular dynamics presented in this paper. Its subsections are as follows: 2.1 provides a brief overview of the Lennard-Jones potential; 2.2 describes how this potential is used to calculate the force on a given point; 2.3 introduces the velocity Verlet method and discusses the equations of motion used in the dynamics simulations, and 2.4 explains how the nanotube group can vary with time.

The third section focuses on the results and analysis of the simulations while Section 4 presents possible avenues of future exploration. Finally, Sections 5 and 6 provide an overview of the software tools used in the simulations and the parameters for the figures shown throughout the paper.

1 Generating Objective Structures

Orthogonal matrices, rotations and affine orthogonal groups play a salient part in the formation of objective structures. Moreover, specific groups of isometries need to be utilized to ensure that the points in the structure remain discrete while maintaining the necessary symmetry. In particular, objective structures consist of every element of a discrete subgroup G of the affine orthogonal group multiplied by every element of a finite set of points $X_0 = \{\mathbf{x}_1 \dots \mathbf{x}_M\}$ in $\mathbb{R}^3$.

1.1 Orthogonal Matrices and Rotations

An orthogonal matrix is a square matrix with orthonormal columns, i.e. the columns are orthogonal and normalized. Every orthogonal matrix, U, is invertible and its transpose is equal to its inverse, $U^T = U^{-1}$. Moreover, if the matrix is $n \times n$, then its columns form an orthonormal basis of $\mathbb{R}^n$.

Orthogonal transformations possess a set of properties that allow for a perfect representation of objective structures. One of these properties is the preservation of dot products. For instance, if $\mathbf{x}$ and $\mathbf{y}$ are two n-dimensional vectors and U is an orthogonal $n \times n$ matrix, then

$$U\mathbf{x} \cdot U\mathbf{y} = \mathbf{x} \cdot \mathbf{y}.$$

In other words, orthogonal transformations preserve the length of vectors and the angles between them. This property is essential for the orthogonal matrices' representation of rotations in space, as further described.

It can be easily shown that orthogonal matrices are closed under multiplication and inversion. Thus, they form a group called *the orthogonal group*, denoted by $O(n)$ where n is the dimension of the matrix. The special orthogonal group $SO(n)$ is a subgroup of $O(n)$ consisting of all orthogonal $n \times n$ matrices with determinant $+1$.

Objective structures are examined in 3-dimensional space and are thus directly related to $SO(3)$. If R is a 3×3 matrix such that $R \in SO(3)$ and if R is not the identity matrix, i.e. $R \neq I_3$, then:

- 1 is an eigenvalue of R with geometric and algebraic multiplicity 1.
- The orthogonal transformation $T(\mathbf{x}) = R\mathbf{x}$ is a rotation of space about

a unique line through the origin.

In this case, there always exists an orthonormal basis of $\mathbb{R}^3$ with respect to which R takes the form:

$$\begin{pmatrix} \cos\alpha & -\sin\alpha & 0 \\ \sin\alpha & \cos\alpha & 0 \\ 0 & 0 & 1 \end{pmatrix}$$

Rotations are characterized by an axis and angle of rotation. The matrix above, for example, is a rotation of angle α about the z-axis.

In general, if $R_{e,\theta}$ is an orthogonal matrix representing rotation of an angle θ about an axis defined by the unit vector e, then the following properties apply:

1. $Re = e$.
2. For unit vector u perpendicular to e,
   - $u \cdot Ru = \cos\theta$
   - $u \times Ru = e(\sin\theta)$.

1.2 Affine Orthogonal Groups and Isometries in $\mathbb{R}^3$

An affine orthogonal transformation in $\mathbb{R}^3$, also called an *isometry* of $\mathbb{R}^3$, is a transformation g that maps $\mathbb{R}^3$ to itself, i.e. $g : \mathbb{R}^3 \to \mathbb{R}^3$, and has the form

$$gx = Rx + c$$

where R is a 3×3 real orthogonal matrix and $x, c \in \mathbb{R}^3$. A convenient notation for the elements of the group is $g = (R|c)$.

Affine orthogonal transformations form a group under composition of functions, called the *isometry group* and denoted by Isom(3). The identity in Isom(3) is $g = (I_3|0)$ where 0 is a the zero vector in $\mathbb{R}^3$. Furthermore,

$$(R_1|c_1)(R_2|c_2) = (R_1R_2|R_1c_2 + c_1) \qquad , \qquad (R|c)^{-1} = (R^{-1}| - R^{-1}c)$$

and two big subgroups of the affine orthogonal group are:

- $O(3)$ - the transformations of the form $g = (R|0)$, and
- $\mathbb{R}^3$ - the translations $g = (I|c)$ which form a commutative normal subgroup of Isom(3).

Thus, the affine orthogonal group can be defined as a semidirect product of the orthogonal group and the translation group.

The full affine orthogonal group contains products of rotations, translations and reflections in planes. Transformations of the form $g = (R|c)$ where $R \in SO(3)$ are classical Euclidean motions generated only by rotations and translations. They can be represented by 4×4 block matrices having the following form:

$$T(R|c) = \left(\begin{array}{c|c} R & c \\ \hline 0 & 1 \end{array}\right)$$

where the dimensions of the blocks are as follows:

$$\dim R = 3 \times 3 \qquad \dim c = 3 \times 1 \qquad \dim 0 = 1 \times 3 \qquad \dim 1 = 1 \times 1.$$

Let $g = T(R|c)$. Since g is a 4×4 matrix, translating and rotating a 3-dimensional vector $\mathbf{u}$ using g requires the use of the homogeneous coordinates of $\mathbf{u}$. Thus if $\mathbf{u} = \begin{bmatrix} x & y & z \end{bmatrix}^T$ where $x, y, z \in \mathbb{R}$, then applying g to $\mathbf{u}$ is equivalent to the following operation:

$$\left(\begin{array}{c|c} R & c \\ \hline 0 & 1 \end{array}\right) \begin{bmatrix} x \\ y \\ z \\ 1 \end{bmatrix} = \begin{bmatrix} x' \\ y' \\ z' \\ 1 \end{bmatrix}$$

where $\mathbf{u}' = \begin{bmatrix} x' & y' & z' \end{bmatrix}^T$ is the position of $\mathbf{u}$ after rotation by R and translation by c.

1.3 Discrete Subgroups

Any nonempty set of affine orthogonal transformations that is closed under both multiplication and inversion is said to be a subgroup of the affine orthogonal group. That is, if $g, g' \in G$, then $g^{-1} \in G$ and $gg' \in G$. Furthermore, a subgroup is said to be discrete if no element of the group is

approached in the limit of other elements in the group. Therefore, the elements of a discrete subgroup remain completely separated. Since the points of an objective structure must remain isolated from one another, it is essential to work with discrete subgroups when generating structures.

1.4 The Nanotube Group

An interesting subgroup that is used to generate objective structures to model carbon nanotubes is defined as

$$G_{\tau,\alpha,n} = \{h^i g^j f^k | i \in \mathbb{Z}, j = 0, ..., n-1, k = 0, 1\}$$

where

$$\begin{aligned} f &= (R_{\mathbf{e_1},\pi} \mid (R_{\mathbf{e_1},\pi} - I)\mathbf{x}_1) \\ g &= (R_{\mathbf{e},2\pi/n} \mid (R_{\mathbf{e},2\pi/n} - I)\mathbf{x}_0) \\ h &= (R_{\mathbf{e},\alpha} \mid \tau e + (R_{\mathbf{e},\alpha} - I)\mathbf{x}_0). \end{aligned}$$

The variables $\mathbf{e}$ and $\mathbf{e}_1$ are perpendicular unit vectors in $\mathbb{R}^3$ that determine the orientation of the objective structure in 3-dimensional space. $\mathbf{x}_0$ and $\mathbf{x}_1$ are also elements of $\mathbb{R}^3$ with $\mathbf{x}_0 \perp \mathbf{e}$ and $\mathbf{x}_1$ defining the position of the structure in $\mathbb{R}^3$. The parameters n, α, and τ are all free to be chosen when defining G, such that $n \in \mathbb{Z}$, $\alpha \in \mathbb{R}$ and $\tau \in \mathbb{R} - \{0\}$. The variable n corresponds to the number of points within a layer, τ determines the distance between the different layers, and α is the angular displacement between points of consecutive layers [2]. These parameters affect the interaction between points in the structure as described later in the paper. It is interesting to note that if α is a rational multiple of π, then there exists an element of the nanotube group, a power of h, that is a direct translation. If, however α is an irrational multiple of π, then there are no direct translations in the group.

Each of the three matrices has special properties. The group element f consists of a 180° rotation about the axis defined by $\mathbf{e_1}$ as well as a translation that moves $\mathbf{e_1}$ away from the origin a distance and direction prescribed by $\mathbf{x_1}$, where $\mathbf{x_1} = \mathbf{x_0} + \xi\mathbf{e}$.

The element g includes a rotation of $2\pi/n$ about $\mathbf{e}$. Similar to that of f, the translation element of g moves $\mathbf{e}$ away from the origin a distance and

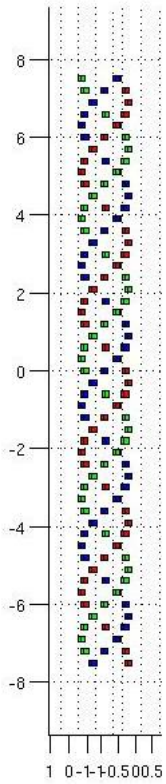

Figure 1: Nanotube with $n = 3$, $\alpha = \frac{\pi}{6}$ and $\tau = 0.3$

direction defined by the vector $\mathbf{x}_0$.

Finally, the group element h includes a rotation about $\mathbf{e}$ and two translations - one that specifies the distance between layers of the nanotube and another that shifts the axis of rotation to a new position described by $\mathbf{x}_0$.

As stated earlier, the vectors $\mathbf{e}$ and $\mathbf{e}_1$ defined in the group determine the orientation of the objective structure in $\mathbb{R}^3$, but they have no effect on the relative positions of the individual points. Thus, the orientation of the rotation axes does not affect the physical behavior of the structure. Therefore, it is convenient to work with objective structures in one set orientation. For all structures shown in this paper, the following definitions apply: $\mathbf{e} = \begin{bmatrix} 0 & 0 & 1 \end{bmatrix}^T$, $\mathbf{e}_1 = \begin{bmatrix} 0 & 1 & 0 \end{bmatrix}^T$, $\mathbf{x}_0 = \begin{bmatrix} 0 & 0 & 0 \end{bmatrix}^T$ and $\xi = 0$ so $\mathbf{x}_1 = \begin{bmatrix} 0 & 0 & 0 \end{bmatrix}^T$.

When G is applied to a single point in $\mathbb{R}^3$, the result is an objective structure similar to that shown in Figure 1. Different objective structures can also be obtained by applying G to a number of points in a fundamental domain [1]. A fundamental domain is defined as a minimal set of points satisfying two conditions: 1) if the group is applied to all points in the set, the entirety of $\mathbb{R}^3$ is generated and 2) it is impossible to obtain points from one another using the group. There exist infinitely many fundamental domains for each discrete affine orthogonal group. The most general formations obtained from the nanotube group are concentric objective structures.

Different structures can also be obtained by using subgroups of the nanotube group. Figures 2 - 6 illustrate objective structures obtained with various subgroups G' of the nanotube group.

2 Molecular Dynamics

Examining the formation of objective structures alone does not provide information for understanding their evolution. In real life, an objective structure consists of atoms or other particles that may exert forces on each other and thus influence the transformation of the whole structure. The simulation of such behavior requires simulation of these forces. The algorithm described in this section uses the Lennard-Jones potential and the velocity Verlet method to simulate the forces and model the dynamics of the structures. A single step of this algorithm involves finding the new position vector of a point after it has moved under the influence of all other points in the

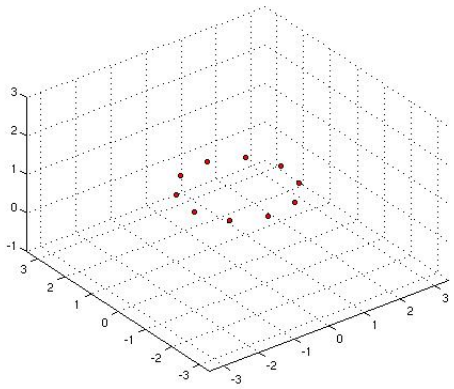

Figure 2: Single Ring
$G' = \{g^i | i = 0, ..., n-1\}$

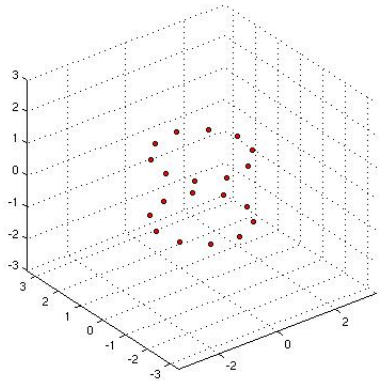

Figure 3: Double Ring
$G' = \{g^i f^k | i = 0, ..., n-1, k = 1, 2\}$

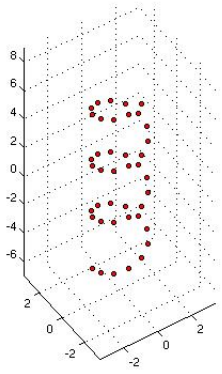

Figure 4: Single Helix
$G' = \{h^j | j \in \mathbb{Z}\}$

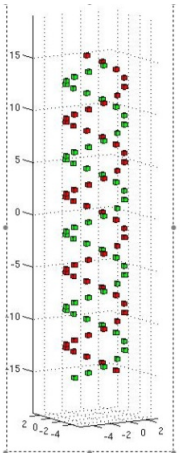

Figure 5: Double Helix
$G' = \{h^j f^k | j \in \mathbb{Z}, k = 1, 2\}$

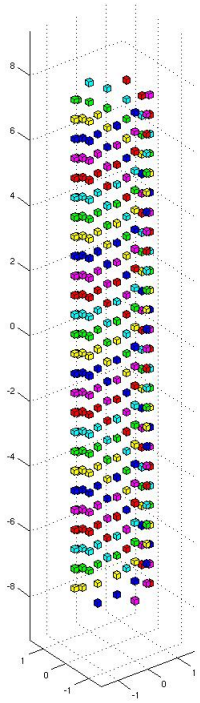

Figure 6: Nanotube
$G' = \{h^j g^i f^k | j \in \mathbb{Z}, i = 0, 1..., n-1, k = 1, 2\}$

structure.

It is important to consider proper initial conditions as well when observing dynamic motion of objective structures. If the initial positions do not place the points in an objective structure, then the system does not evolve as an objective structure. However, if the initial points are properly selected and the initial velocities maintain the symmetry imposed by the group, then the structure is guaranteed to remain an objective structure throughout its evolution. Because of this fact, the system can be simulated by tracking only a finite number of points in a fundamental domain. It is interesting to note also that if the velocities do not have the proper symmetries, then the set may evolve as an objective structure with a changing group or it may lose its objective structure completely.

In the case when the objective structure itself is finite, the force exerted on every point by every other point is calculated and used to simulate the structure's movement. In the case when the structure is infinite, only the points within a certain distance of a particular point are taken into account.

If the structure is generated by a single point, the algorithm described above is applied only to this point. If, however, the structure is formed by a set of points in a fundamental domain, then the algorithm is applied to every point in the set. In both cases, the structure is regenerated after each step by multiplying the generating points by the group elements.

2.1 Lennard-Jones Potential

In order to determine the interacting forces between the points in an objective structure, a potential function is utilized. The simplest and most frequently used potential in computer simulations is the Lennard-Jones potential between a pair of atoms:

$$\phi(\mathbf{w}_1, \ldots) = a \sum_{k \neq l} \left(\frac{\sigma}{|\mathbf{w}_k - \mathbf{w}_l|} \right)^{12} - \left(\frac{\sigma}{|\mathbf{w}_k - \mathbf{w}_l|} \right)^{6}$$

where $\mathbf{w}_k$ and $\mathbf{w}_l$ are vectors describing the positions of points within the objective structure, and σ and a are both positive constants. Although this is an approximate potential, it has the features needed to describe the interactions between closed shell atoms: namely, a strong repulsive short range

interaction, a long range van der Waals attraction, and a potential well. In real physical systems, a and σ depend on the type of the particles - a represents the depth of the potential well, and σ is the distance at which the interparticle potential is zero. Also, the potential reaches its minimum at a distance of $\sqrt[6]{2}\sigma$ between the particles. As described in the next section, the forces on each point are dependent on the potential function and are thus sensitive to a and σ.

2.2 Calculating Forces from the Potential Function

To derive the equations for the forces on a point whose position is given by the vector $\begin{bmatrix} x & y & z \end{bmatrix}^T$, the gradient of the potential function given above must be found. Because the partial derivative of the potential must be taken with respect to the x, y, and z coordinates, it is convenient to rewrite the potential as

$$\begin{aligned} \phi &= a\sigma^{12}\sum((x-x_i)^2+(y-y_i)^2+(z-z_i)^2)^{-6} \\ &\quad -a\sigma^6\sum((x-x_i)^2+(y-y_i)^2+(z-z_i)^2)^{-3}. \end{aligned}$$

Thus, the partial derivative with respect to x_i is:

$$\begin{aligned} \frac{\partial\phi}{\partial x_i} &= 6a\sigma^6\sum\left[\frac{2\sigma^6(x-x_i)}{\left[(x-x_i)^2+(y-y_i)^2+(z-z_i)^2\right]^7}\right. \\ &\quad \left.-\frac{(x-x_i)}{\left[(x-x_i)^2+(y-y_i)^2+(z-z_i)^2\right]^4}\right]. \end{aligned}$$

A similar result is obtained for the y and z components of the gradient, which together with x_i form the negative y, z and x components of the net force acting on the point of interest from all other points. That is, $F = -\nabla\phi$. This force is then used to find the acceleration of the point mass and determine its new velocity and position in space. In the model implemented here, discrete time steps are taken, though the process is continuous. Through implementation of the Verlet method, a reasonable simulation can be presented in many cases, however there are still significant sources of error that result in drastic misrepresentations of real physical systems.

For a structure with a finite number of points, the effect of all points in the structure can be taken into account. However, for infinite structures, this

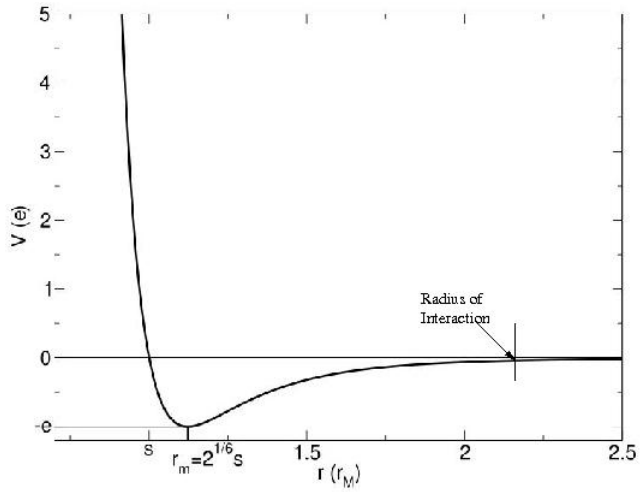

Figure 7: Lennard-Jones Potential Function: radius versus potential

would certainly be impossible. Fortunately, as the distance between points increases to infinity, both the value of the potential function and the force that the point masses exert on one another approach zero, as shown in Figure 7. Because of this property, when evaluating the forces for infinite objective structures, it is useful to specify a reasonable radius of interaction such that only points within this radius will be considered to interact significantly with the point of interest. A reasonable value for this radius in terms of σ can be found by minimizing the potential function and selecting a value sufficiently greater than this minimum. In the following analyis, the radius is chosen such that all points generated in simulations of the infinite structures are taken into account.

2.3 Velocity Verlet Method

The velocity Verlet method is used in the dynamic simulations of the structures. This method is the most widely used algorithm to compute trajectories of particles under the influence of some force. It is more accurate than the Euler method, but still uses finite timesteps which means that it is discrete rather than continuous. Following is a description of the method.

Given the initial position x_0 and the initial velocity v_0, the force on the point mass is calculated using the Lennard-Jones potential. Let F_n be the force at the end of the n^{th} time step. Then the half-step velocity is:

$$v_{n+\frac{1}{2}} = v_n + \Delta t \frac{F_n}{2m}$$

where F is the force, t is time, v is the velocity and m is the mass of the particle. The position for the next time step is calculated using the half-step velocity instead of the current velocity. This makes it possible to compute an extra term in the Taylor polynomial of position, hence making it more accurate:

$$x_{n+1} = x_n + \Delta t v_{n+\frac{1}{2}}.$$

The force at the next time step can then be calculated as:

$$F_{n+1} = F(x_{n+1}).$$

Eventually, the full time-step velocity is obtained by using the above force and the half time-step velocity.

$$v_{n+1} = v_{n+\frac{1}{2}} + \Delta t \frac{F_{n+1}}{2m}.$$

2.4 Time Variance in the Nanotube Group

Simulation of the dynamics of objective structures is not exhausted by applying forces to generate movement. The algorithm described above involves regeneration of the whole structure after each step. Therefore, varying the matrices generating the structures produces a different type of transformation.

With linear time variance, τ, x_0 and x_1 are calculated as:

$$\begin{aligned} \tau(t) &= \tau_0 + tu && \text{where } u \in \mathbb{R} \\ \mathbf{x}_0(t) &= \mathbf{x}_0 + t\mathbf{v} && \text{where } v \in \mathbb{R}^3 \\ \mathbf{x}_1(t) &= \mathbf{a} + t\mathbf{b} && \text{where } \mathbf{a}, \mathbf{b} \in \mathbb{R}^3 \end{aligned}$$

where $\mathbf{x}_0(t)$ and $\mathbf{x}_1(t)$ are Euclidean displacements. This linear time variance matches the evolution predicted by the forces from the Lennard-Jones

potential for suitable initial conditions.

The purpose of the analysis in this paper is to examine the evolution of objective structures. Therefore, the main focus lies on transformations that affect only the relative distances between points and not the position of the structure in space. Thus, the analyzed time variance in groups involves only changes in the translational element of the matrix h as defined in Section 1.4, i.e. changes in the parameter τ (the distance between consecutive rings).

3 Results and Analysis

A good measure of the behavior of objective structures is the minimum radius that the cylindrical nanotube achieves during its evolution. Due to interparticle forces, in many cases the structure expands and contracts. Figure 8 shows typical plots of the radius of a structure generated from a single point.

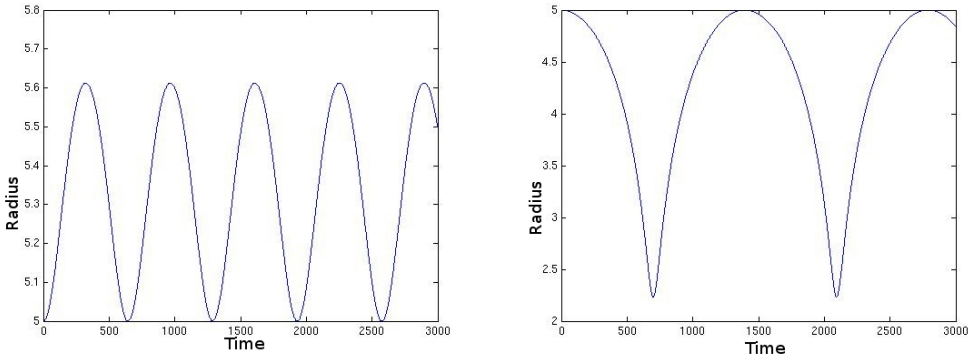

Figure 8: Typical plots of the radius of a nanotube versus time under the influence of the Lennard-Jones potential

It is observed that in many cases the radius oscillates between two fixed extremes when the structure is left under the influence of the Lennard-Jones potential. When the radius achieves its minimum value, the velocity of the particles becomes zero and changes direction. This means that the energy of

the system is purely potential and allows for easy comparison between different structures. The minimum radius can be affected by several parameters, some of which are discussed below.

For simplicity, when modeling the dynamics of objective structures the matrix f as defined in Section 1.4 is not applied.

3.1 Overview of Parameters

Following is a brief overview of the main parameters used in the analysis.

n number of points in a ring, or equivalently, number of helixes in a nanotube structure; as n grows larger, points on every ring grow closer together and feel greater repulsion force; hence, the structure expands rapidly.

τ displacement between consecutive layers in the structure

α angular displacement between corresponding points in consecutive layers

$\mathbf{x_0}$ initial position of the generating point, which also determines the initial radius of the structure; if $\mathbf{x_0}$ is sufficiently small, then points in a ring repel one another immediately; if $\mathbf{x_0}$ lies on the axis of rotation, the result is a single line of translated points and the forces are all parallel to this line

$\mathbf{v_0}$ initial velocity of generating point

3.2 The Effect of τ

When generating an objective structure from a single point, the displacement between layers of the structure, τ, is inversely related to the force exerted on the point from which the structure is generated, $\mathbf{x}_0$. This relationship has the effect of increasing the force on $\mathbf{x}_0$ if τ decreases and vice

versa. The reason for this behavior is the fact that a smaller τ value results in a closer grouping of points and therefore the distance between $\mathbf{x}_0$ and the points on other layers of the structure is considerably shorter. Because the forces are entirely dependent on the distance between points, there is a considerable increase in the force exerted on $\mathbf{x}_0$. The resulting behavior is observed by examining the correlation between τ and the tube radius. Figure 8 shows how the tube radius changes over time (the same pattern appears for structures generated with different input parameters where $\alpha \neq 0$). As it can be seen in the graph, the structure expands and contracts while obtaining a maximum and a minimum radius. To explore the effect of the displacement between layers of the structure on the forces, τ is plotted against the minimum radius (Figure 9(a)) and against the number of time steps necessary for reaching the minimum radius (Figure 9(b)). In the simulations analyzed in this section the objective structures are generated by a single point which is initially at rest, i.e. $\mathbf{v}_0 = \begin{bmatrix} 0 & 0 & 0 \end{bmatrix}^T$.

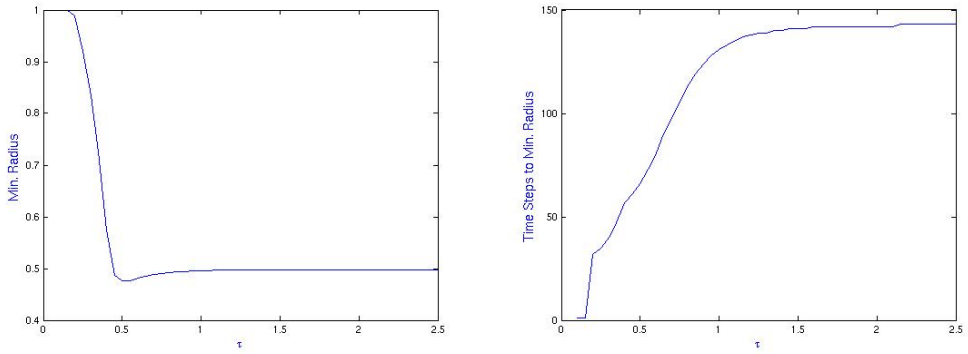

(a) τ versus minimum radius (b) τ versus time steps

Figure 9: Dependence between τ and (a) the minimum radius and (b) the number of time steps necessary to obtain the miniumum radius.

Note that for very small values of τ the repulsive force is initially strong enough that the structure starts expanding immediately and the initial radius appears to be the minimum radius. For a larger τ, the distance between points on adjacent layers is greater which results in a weaker repulsive force thus allowing the structure to contract intially before expanding. A structure with a smaller τ parameter will obtain its minimum radius more quickly than a structure with a larger τ, as seen in Figure 9(b). It is apparent that,

once τ increases beyond a certain value, the minimum radius approaches a constant. At the same time, the number of time steps necessary for reaching this minimum radius also approaches a constant. It has been observed in several cases that the constant value the minimum radius approaches is equal to σ. An interesting property is also that the absolute minimum of the plot in Figure 9(a) is obtained when τ is equal to σ, one of the two parameters in the Lennard-Jones potential (see Section 3.1 for exact parameter values). These results have been verified for various values of σ where $\alpha \neq 0$ (see Section 3.4).

3.3 The Effect of a Time Variant Group

In the following analysis the structures are generated by a single point that is initially at rest and u is a constant where $\tau = \tau_0 + u * t$ with t being time.

Similar to the analysis in Section 3.2, the effect of the parameter u on the structure is examined by comparing u to the minimum tube radius and to the time steps necessary for achieving the minimum radius. Surprisingly, a linear time variance in the group does not significantly affect the minimum radius: for instance, when u varies from 1 to 20, the range of the radius values is only .0009. On the other hand, Figure 10 shows that as u increases, the number of time steps necessary for reaching the minimum radius also increases while approaching a fixed value.

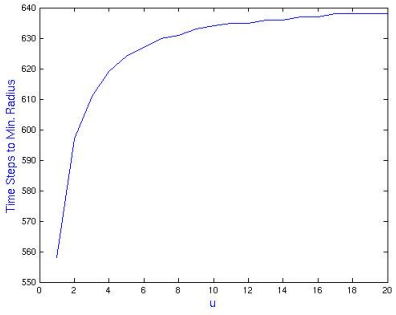

Figure 10: Effect of linear time variance on time necessary for reaching minimum tube radius

It has been observed also that when u is less than 1, the objective structure does not maintain consistent pulsating behavior. Rather, the radius decreases to a minimum and then continually increases, never obtaining a maximum value. Considering the apparent stability in the behavior of objective structures for different values of τ, as analyzed in Section 3.2, this result is very surprising.

3.4 The Effect of α

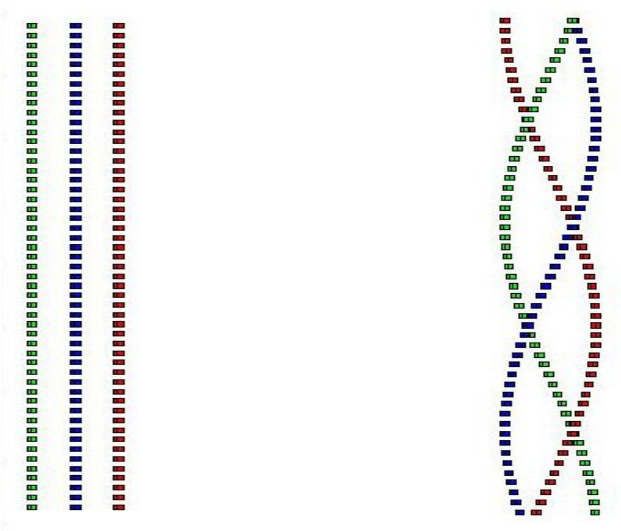

(a) $\alpha = 0$ (b) $\alpha = 0.2$

Figure 11: Effect of variation of α

The parameter α is the measure of the angular displacement between two consecutive rings of the nanotube. If α is zero, then the rings stack neatly on top of each other, with corresponding points in the rings lying in a straight line parallel to the axis of rotation. For any other value, each ring is a rotated version of the one below with the angle of rotation being α. For $\alpha = \frac{\pi}{n}$, each point is midway between the two closest points in the ring above it, since the angle between two consecutive points in a ring is $\frac{2\pi}{n}$. Hence the results

would be symmetric about this value of α.

The following results are obtained by varying α in different scenarios. Eight equally spaced values between 0 and $\frac{\pi}{n}$, inclusive, are chosen for α, where n is the number of particles in a ring of the structure. The parameters for the Lennard-Jones potential are kept constant with $a = 3$, $\sigma = 0.5$ and $\tau = 0.3$.

Starting with $n = 5$, initial position and velocity of the generating point as $\begin{bmatrix} 5 & 0 & 0 \end{bmatrix}^T$ and $\begin{bmatrix} 0 & 0 & 0 \end{bmatrix}^T$ respectively, the following plot of minimum radius versus alpha is obtained:

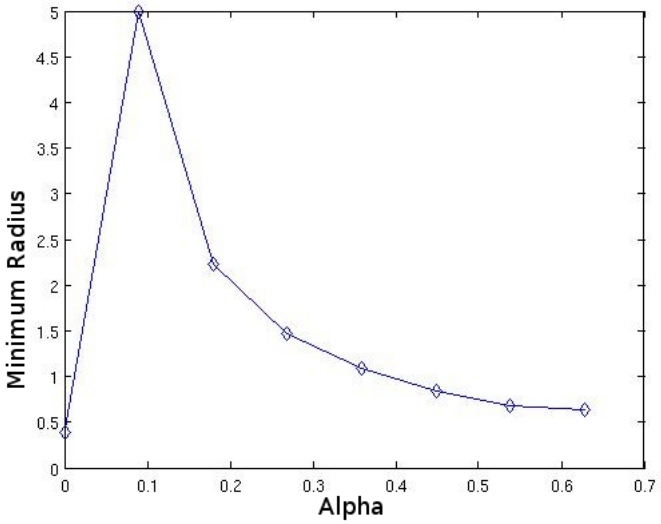

Figure 12: Variation of minimum radius versus α

Figure 12 shows that there is a discontinuity at $\alpha = 0$. The minimum radius is lowest for this value, but increases suddenly and significantly for α slightly greater than 0. It then drops off and achieves a local minimum for $\alpha = \frac{\pi}{n}$.

Figures 13(a) and 13(b) show a similar trend for different initial parameters. In Figure 13(a), $n = 5$ and initial position and velocity of the generator point are $\begin{bmatrix} 5.1 & 0 & 0 \end{bmatrix}^T$ and $\begin{bmatrix} -0.5 & 0 & 0 \end{bmatrix}^T$ respectively. In Figure 13(b), $n = 6$ and initial position and velocity of the generator point are $\begin{bmatrix} 6 & 0 & 0 \end{bmatrix}^T$ and $\begin{bmatrix} -0.5 & 0 & 0 \end{bmatrix}^T$ respectively.

These figures suggest that the structure has low minimum radii for α

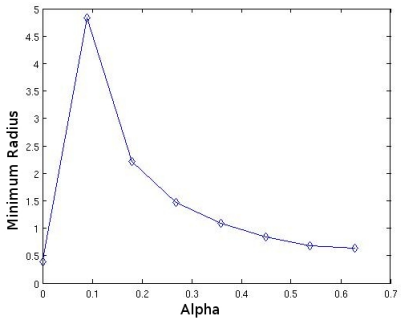

(a) $n = 5$ and small inward initial velocity

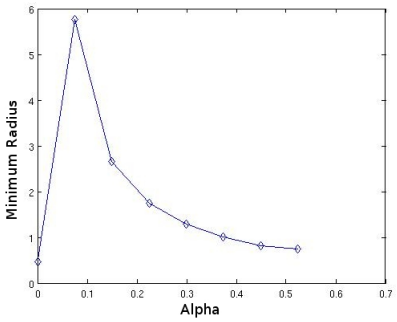

(b) $n = 6$ and small inward initial velocity

Figure 13: Variation of minimum radius versus α

equal to 0 and $\frac{\pi}{n}$. The minimum radius increases gradually as α is varied from $\frac{\pi}{n}$ to 0. At $\alpha = 0$ there is a disconuinity. The particles in the structure can come much closer to each other for $\alpha = 0$ and for $\alpha = \frac{\pi}{n}$ compared to other values of α. Thus, in such situations, the potential energy of the system would be very high. However, these results are influenced by the value of τ. The effect of changing τ is shown in figure 14.

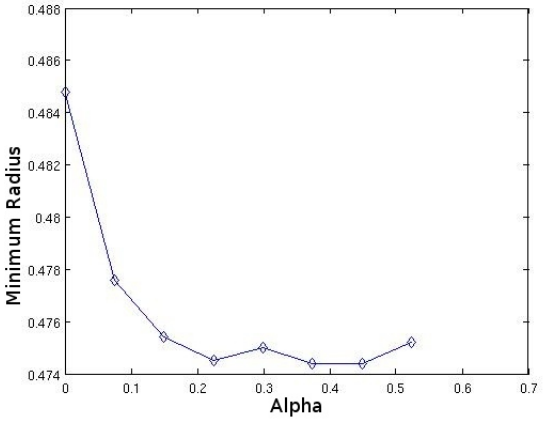

Figure 14: Variation of minimum radius versus α for $\tau = 0.6$

Figure 14 shows that for τ greater than a specific value, the minimum radius of the structure decreases with increasing α, with no discontinuity at $\alpha = 0$. The value of τ above which this happens is $\sqrt[6]{2}\sigma$, and for $\sigma = 0.5$

this is 0.56. This is the distance of minimum potential in the Lennard-Jones model, and the force between two particles at this distance is zero. The reasons for this behavior can be understood further from figure 15.

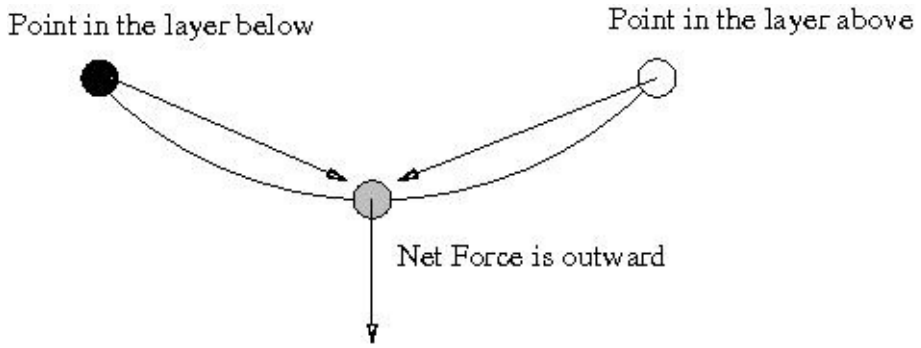

Figure 15: Analysis of forces on the generating point for $\tau < \sqrt[6]{2}\sigma$

For $\alpha = 0$, the points obtained by applying the nanotube group element h on the generating point are collinear. Due to this symmetry, the forces on the generator point due to this part of the structure cancel out. The other points of the structure, obtained by applying the group element g are very far and have a small attractive influence on it, causing the structure to shrink gradually. On slightly increasing α, the points that were collinear now form a spiral. As shown in figure 15, for $\tau < \sqrt[6]{2}\sigma$, the points above and below the generating point exert a large repulsive force, as they are closer than the distance of minimum potential. This causes the structure to expand and increases its minimum radius. However, if $\tau > \sqrt[6]{2}\sigma$, all points attract the generating point and the structure shrinks. Hence the minimum radius is smaller than when $\alpha = 0$.

Thus, it can be concluded that the minimum radius of the structure during its evolution is lowest for $\alpha = \frac{\pi}{n}$ when $\tau > \sqrt[6]{2}\sigma$. However, for $\tau < \sqrt[6]{2}\sigma$, it is lowest for $\alpha = 0$ and has a local minimum for $\frac{\pi}{n}$.

4 Future Directions

During the period of this research, we answered a few questions about Objective Structures and raised some interesting new ones. Here we present some issues that suggest further investigation.

For the simulations studied in this paper, a discrete time-step for the Verlet method was used. This is only an approximation and might diverge from real life behavior over long periods of time. An improvement might be to reduce the time-step, but this approach is limited by computing power. Introducing a damping factor would make simulations more realistic, as physical systems lose energy over time. This would also ensure that the structure does not expand into a gas due to high initial energy.

Another improvement could lie in the model used to calculate the forces between the particles. The Lennard-Jones Potential used in this paper is simplistic and may not apply to all kinds of particles. Even where the model is applicable, it might be interesting to simulate the structures with values of parameters a and σ specific to the pairs of particles in question, instead of fixed values for all points. A more general model that takes into account such considerations would provide further insight into the behavior of these structures.

An important facet of objective structures that needs to be explored is the variety of groups beyond the nanotube group. One group that has great practical importance is the icosahedral group. This group is used to generate buckyballs, which have several interesting properties and applications in physics and chemistry. The lattice group generates lattice layers in space and is another important group that merits further study.

One important experiment that could not be studied due to brevity of the research period was the effect on angular velocity in the case of objective structures generated from multiple points in a fundamental domain for the nanotube group. For structures generated from a single point, it was observed that any initial angular motion gradually disappears. However, simulations on concentric tubes indicated that angular displacement between the tubes could augment angular velocity and make the entire structure rotate. It would be interesting to study the relationship between the initial configuration of the system and the angular velocities achieved by it.

5 Methodology

MATLAB has been used to simulate the motions of objective structures analyzed in this paper. This section discusses the basic methods and MATLAB functions used for calculation and visualization with this software.

Calculations:

- The function *makehgtform* is used to generate rotation and translation matrices (the resulting matrices are 4×4, which requires the use of homogeneous coordinates for vectors).
- Nested loops are used to apply the whole nanotube group to a single point.
- The partial derivatives of the Lennard-Jones potential function are entered manually into the programs to resolve efficiency issues.
- To avoid computation error, the uniqueness of every point in a structure is verified using the function *unique*.
- When calculating the force on a point, it is sometimes necessary to require that only points beyond a certain tolerance radius interact with the point of interest. This is needed because of error introduced through calculations in the programs that cause the structures to exhibit unusual behavior. For the presented simulations, the tolerance distance is specified to be 10^{-5}.

Display:

- Rather than using graphics objects, the points in the simulated objective structures are displayed by markers or cubes generated with the *patch* function.
- When plotting cubes with the *patch* function, it is possible to specify the cubes within one helix to be the same color, thus making different helices in a structure different colors. This allows motion to be more apparent when observing how the structures evolve. A similar procedure can be followed when generating structures with markers using

the *plot3* function. For the sake of program efficiency, it is convenient to use the *set* function when updating the images in these cases.

- The functions *set* and *drawnow* are used to allow for manually rotationing the structures while the programs are running.

6 Parameters of Figures

Figure	n	τ	α	σ	a	$\mathbf{x}_0$	$\mathbf{v}_0$
1	3	0.3	$\frac{\pi}{6}$	-	-	$\begin{bmatrix} 1 & 0 & 0 \end{bmatrix}^T$	-
2	10	-	-	-	$\begin{bmatrix} 1 & 0 & 0 \end{bmatrix}^T$	-	-
3	10	-	-	-	$\begin{bmatrix} 1 & 0 & 1 \end{bmatrix}^T$	-	-
4	1	0.3	$\frac{\pi}{6}$	-	-	$\begin{bmatrix} 1 & 0 & 0 \end{bmatrix}^T$	-
5	1	0.3	$\frac{\pi}{6}$	-	-	$\begin{bmatrix} 1 & 0 & 1 \end{bmatrix}^T$	-
6	5	0.3	$\frac{\pi}{6}$	-	-	$\begin{bmatrix} 1 & 0 & 1 \end{bmatrix}^T$	-
9	6	$0.1, \ldots, 2.5$	$\frac{\pi}{6}$	0.5	3	$\begin{bmatrix} 1 & 0 & 0 \end{bmatrix}^T$	$\begin{bmatrix} 0 & 0 & 0 \end{bmatrix}^T$
10	6	0.3*	$\frac{\pi}{6}$	0.5	3	$\begin{bmatrix} 1 & 0 & 0 \end{bmatrix}^T$	$\begin{bmatrix} 0 & 0 & 0 \end{bmatrix}^T$
12	5	0.3	$0, \ldots, \frac{\pi}{n}$	0.5	3	$\begin{bmatrix} 5 & 0 & 0 \end{bmatrix}^T$	$\begin{bmatrix} 0 & 0 & 0 \end{bmatrix}^T$
13(a)	5	0.3	$0, \ldots, \frac{\pi}{n}$	0.5	3	$\begin{bmatrix} 5.1 & 0 & 0 \end{bmatrix}^T$	$\begin{bmatrix} -0.5 & 0 & 0 \end{bmatrix}^T$
13(b)	6	0.3	$0, \ldots, \frac{\pi}{n}$	0.5	3	$\begin{bmatrix} 6 & 0 & 0 \end{bmatrix}^T$	$\begin{bmatrix} -0.5 & 0 & 0 \end{bmatrix}^T$
14	6	0.6	$0, \ldots, \frac{\pi}{n}$	0.5	3	$\begin{bmatrix} 6 & 0 & 0 \end{bmatrix}^T$	$\begin{bmatrix} -0.3 & 0 & 0 \end{bmatrix}^T$

7 Acknowledgements

This paper is a result of the Interdisciplinary Research Experience for Undergraduates organized by the Institute for Mathematics and Its Applications (IMA) at University of Minnesota, Twin Cities from June 28 to July

31, 2009. We gratefully acknowledge the IMA for providing us with this opportunity.

This research is inspired by the pioneering work of Prof. Richard James, to whom we would like to extend a special thanks. We would also like to thank our advisor Prof. Daniel Flath, and our postdoctoral mentor Hannah Callender for their invaluable guidance and insight. Their constant presence and unwavering support helped us get through any obstacles that we faced.

References

[1] James, R.D. Objective Structures, *Journal of the Mechanics and Physics of Solids* **54** (2006) 2354-2390

[2] Dayal, K., James, R.D. Non-equilibrium Molecular Dynamics for the Viscometric Characterization of Bulk Materials and Nanostructures, *Journal of the Mechanics and Physics of Solids* (2009)